Skeletal Radiology (2020) 49:1965–1975
https://doi.org/10.1007/s00256-020-03508-7

SCIENTIFIC ARTICLE

Comparison of 3D X-ray tomography with computed tomography in patients with distal extremity fractures

Anna L. Falkowski[1,2] · Balazs K. Kovacs[1] · Fides R. Schwartz[1] · Robyn M. Benz[1] · Bram Stieltjes[1] · Anna Hirschmann[1]

Received: 20 March 2020 / Revised: 29 May 2020 / Accepted: 7 June 2020 / Published online: 18 June 2020

Abstract

Objective To compare fracture detection, image quality, and radiation dose in patients with distal extremity fractures using 3D tomography and computed tomography (CT).

Materials and methods IRB approval was obtained including informed consent for this prospective study from June to December 2016. Patients diagnosed with an acute fracture at CT were consecutively scanned on the same day using 3D tomography. Anatomical location (effected bone and location within the bone) and morphological characteristics of fractures (avulsion, articular involvement, mono- vs. multifragmented, displacement), visibility of bone/soft tissue structures, and image quality were assessed independently by two blinded readers on a 5-point Likert scale. Dose-length-product (DLP; mGy*cm) was compared between both modalities. Descriptive statistics, Wilcoxon signed rank test ($P < 0.05$), Student's t test ($P < 0.05$), and Cohen's kappa (κ) for interreader reliability were calculated.

Results In 46 patients (28 males; 18 females; mean age, 53 ± 20 years) with 28 hand/wrist and 18 foot/ankle examinations, 86 out of 92 fractures were diagnosed with 3D tomography compared with CT. No false-positive finding occurred at 3D tomography. The six missed fractures on 3D tomography were five avulsion fractures of the carpals/metacarpals or tarsals/metatarsals, respectively, and one nondisplaced fracture of the capitate. Interreader agreement of anatomical location and morphological characteristics was substantial to almost perfect for upper (κ = 0.80–0.96) and lower (κ = 0.70–0.97) extremity fractures. Visibility of bone and soft tissue structures and image quality were slightly inferior using 3D tomography compared with CT (upper extremity $P < 0.001$–0.038 and lower extremity $P < 0.001$–0.035). DLP of a comparable scan coverage was significantly lower for 3D tomography ($P < 0.001$) for both upper (3D mean, 19.4 ± 5.9 mGy*cm; estimated CT mean, 336.5 ± 52.2 mGy*cm) and lower extremities (3D mean, 24.1 ± 11.1 mGy*cm; estimated CT mean, 182.9 ± 6.5 mGy*cm). Even the highest DLP with 3D tomography was < 30% of the mean estimated CT dose of a comparable area of coverage.

Conclusion Fracture assessment of peripheral extremities is reliable utilizing a low-dose 3D tomography X-ray system, with slightly reduced image quality.

Keywords Trauma · Emergency · Radiation dosage · Ankle · Wrist · Computed tomography · 3D X-rays

✉ Anna L. Falkowski
falkowski.anna@gmail.com

Balazs K. Kovacs
balazskrisztian.kovacs@usb.ch

Fides R. Schwartz
fides.schwartz@duke.edu

Robyn M. Benz
roebe@gmx.net

Bram Stieltjes
bram.stieltjes@usb.ch

Anna Hirschmann
anna.hirschmann@usb.ch

[1] Department of Radiology, University Hospital Basel, University of Basel, Petersgraben 4, 4031 Basel, Switzerland

[2] Department of Radiology, Orthopedic University Hospital Balgrist, University of Zurich, Forchstrasse 340, 8008 Zurich, Switzerland

Abbreviations

CT	Computed tomography
3D	Three dimensional
cm	Centimeter
kVp	Kilovolt peak
mAs	Milliampere-seconds
DLP	Dose-length-product
n	Number

Introduction

Fractures of the distal extremities are common and need adequate therapy to avoid complications such as malalignment, stiffness, and posttraumatic osteoarthritis [1]. Treatment options vary, and the choice of fracture treatment is based on the clinical presentation, patient's requirement, presence and degree of displacement of bone fragments, and articular surface involvement [2]. Radiography is usually the diagnostic imaging tool of choice. However, computed tomography (CT) can be a useful additional examination to detect or exclude occult fractures as well as for surgical planning [3]. Additional information of CT includes the exact assessment of intraarticular fractures, accuracy of the fracture extension, and occult fractures on radiographs due to superimposed adjacent bony structures [2, 3]. However, there are disadvantages to the application of CT for fracture diagnosis, e.g. substantially higher costs, higher radiation dose, and larger spatial demands [4]. Thus, some authors studied the use of cone-beam CT to address these issues with promising results [2, 5] since a system that would integrate the low radiation dose of radiography with the high resolution of CT would be ideal for fracture assessment.

A multifunctional X-ray system with a twin robotic technology permits the acquisition of radiographs, fluoroscopy, and 3D tomography within one unit. This 3D tomography acquires images in a cone-beam CT scanning mode. However, it has only been evaluated by experimental and cadaveric studies [6–9]. These cadaveric studies only investigated parameters such as image quality and radiation dose, but have not investigated pathologies such as fracture detection. Thus, the purpose of our study was to evaluate fracture analysis, image quality, and radiation exposure of 3D tomography in clinical performance using this twin robotic X-ray system compared with CT in patients with distal upper and lower extremity fractures in an emergency setting. Our hypothesis was that image quality is inferior with 3D tomography, but the radiation dose is lower and fracture detection is comparable with CT.

Materials and methods

Patients and image acquisition

All patients were prospectively enrolled after IRB-approval from June to December 2016. Informed consent was obtained from all individual participants included in the study. Patients from the emergency department, who needed a CT, because their symptoms did not match the radiographic findings or needed a CT for surgical planning, were included if an acute fracture of the distal extremities was diagnosed on CT. Patient inclusion was performed by a fellowship-trained musculoskeletal radiologist, who did not perform image analysis. The included patients were additionally scanned using 3D tomography. Distal upper extremity scans included the wrist and hand and distal lower extremity scans included the ankle and foot. Both scans were performed on the same day. Exclusion criteria were age of patients < 18 years and missing informed consent. An inability of the patient to examine the upper extremity placing the arm above the head on CT was an exclusion criterion. Otherwise, the patient would have to be examined with the hand placed on or next to the body, which might have impacted the comparability with 3D tomography due to impaired image quality and increased radiation dose on CT. Fixation devices, e.g. cast or external fixation, were not exclusion criteria.

3D tomographies of the extremities were acquired using a twin robotic X-ray unit (Multitom Rax, Siemens Healthineers, Erlangen/Germany) with reformats in three orthogonal planes. The side trajectory with 192 projections was utilized to examine the distal upper extremities (tube voltage, 70 kVp; tube current, 21.2–52.2 mAs; scan time, 20 s; field of view, 23 cm). Here, the patient was in supine position and the examined arm was 90° abducted.

The table trajectory with 160 projections was used to examine the distal lower extremities (tube voltage, 70 kVp; tube current, 27.1–107.8 mAs; scan time, 20 s; field of view, 23 cm). The patient was placed in supine position and the foot was examined in slight plantarflexion to minimize cone-beam artifacts; the contralateral leg was flexed and outside the field-of-view.

CT examinations were performed using a 128-slice scanner (Somatom AS+, Siemens Healthineers, Erlangen/Germany) with reformats in three orthogonal planes. Distal upper extremity scans (fixed tube voltage, 120 kVp; tube current, 150 mAs; scan range, 9–26 cm) were performed with the patient in prone position placing the examined arm above the head.

Distal lower extremity scans (fixed tube voltage, 120 kVp; tube current, 100 mAs; scan range, 12–28 cm) were performed in supine position and the ankle was placed at 90° dorsal extension; the contralateral leg was flexed. This position was chosen to align the ankle joint.

Image analysis

Images were extracted from the PACS system and analyzed anonymously using OsiriX (Pixmeo, Geneva/Switzerland). The 3D tomographic and CT data sets were evaluated on 3D multiplanar reconstructions. Interpretation tools, e.g. magnification and contrast, were available to use. The reading was performed independently and randomly by two radiologists, a musculoskeletal expert 7 years following board examination and a 4th year resident, both blinded to the diagnosis of fracture location. The readout of the 3D tomography was performed first, and the CT readout performed second with a re-randomized patient order. The readers had a chronologic break of 2 weeks between the readouts of both modalities. Fracture evaluation was performed analyzing location (epiphyseal, metaphyseal, diaphyseal, proximal vs. distal) and number of fragments (monofragmented/multifragmented), as well as articular involvement (yes/no), avulsion (yes/no), and displacement (yes/no). Qualitative evaluation of bone (visibility of trabeculae and cortices of the capitate and talus, respectively) and soft tissue structures (differentiation of muscles and tendons from fat) as well as subjective image quality (noise, overall image quality, artifacts) was assessed on a 5-point Likert scale. The Likert scale was encoded as followed for all criteria but artifacts: 1 = excellent, 2 = good, 3 = fair, 4 = poor, 5 = inadequate; and for artifacts: 1 = no artifacts, 2 = minor artifacts without influence of image assessment, 3 = moderate artifacts without influence of image assessment (diagnosis still possible), 4 = heavy artifacts with influence of image assessment (only partial diagnosis possible), and 5 = severe artifacts making diagnosis impossible. Conflicting findings of fracture evaluation were resolved by consensus reading between both radiologists. No consensus reading was performed for qualitative evaluation.

Additionally, a retrospective review of available radiographs was performed.

The dose-length-product (DLP; mGy*cm) adapted to scan range was compared between both modalities.

Statistical analysis

Descriptive statistics and Wilcoxon signed rank test (threshold of significance $P < 0.05$) were used to report fracture, qualitative image, and radiation exposure analysis. Cohen's kappa was used to measure the interreader reliability regarding fracture and qualitative analysis. Student's t test (threshold of significance $P < 0.05$) was performed for subgroup analysis regarding differences between patients without and with cast, as well as patients without and with external fixation. Cohen's kappa value of 0.81–1.00 is considered (almost) perfect, 0.61–0.80 substantial, 0.41–0.60 moderate, 0.21–0.40 fair, 0–0.20 slight, and < 0 poor [10]. All statistics were performed using SPSS software (version 22.0; SPSS, Chicago, USA).

Results

Demographics and fracture analysis

Forty-six patients (28 males; 18 females; mean age, 53 ± 20 years) were included in the study. Fifteen out of 18 CT scans of the distal lower extremities were performed in the supine position with the ankle placed at 90° dorsal extension. Three patients could not tolerate this position, and the foot was examined in slight plantarflexion. Seven patients of the upper extremity group had a cast, and four of the lower extremity group had an external fixation present at the time of both scans.

The consensus reading was required for five interreader disagreements, one at the hand and four at the foot: (1) nondisplaced fracture of the middle phalanx of the fifth finger; (2) nondisplaced avulsion of the navicular bone; (3) slightly displaced avulsion fracture of the calcaneus; 4) displaced base fracture of the second metatarsal bone; 5) in a patient with external fixation, avulsion fractures were interpreted by reader 1 to be attributed to the tibia and by reader 2 to the fibula. In the consensus, all of the identified fractures were considered as fractures. Additionally, in the last patient, the avulsion fractures were attributed to both the tibia and fibula.

Following the consensus reading, 28 patients with fractures of the distal upper, i.e. hand and wrist, and 18 patients with fractures of the distal lower extremity, i.e. foot and ankle, were scanned (Table 1). In total, 92 fractures were present on CT with 46 each of the upper and lower distal extremities, respectively. Single fractures were present in 18 patients (14 upper/4 lower distal extremities), 2 simultaneous fractures were present in 16 patients (8 upper/8 lower distal extremities), 3 simultaneous fractures in 8 patients (4 upper/4 lower distal extremities), 4 simultaneous fractures in 2 patients (1 upper/1 lower distal extremities), and 5 simultaneous fractures in 2 patients (0 upper/2 lower distal extremities). Eighty-six of these 92 fractures (93%) were visible on 3D tomography (43 of 46 fractures of each upper and lower distal extremities; Figs. 1 and 2). Six fractures (7%) in three patients were missed on 3D tomographic images (Table 1): avulsion fractures of the triquetrum ($n = 1$), 2nd metacarpal ($n = 1$; Fig. 3), lateral cuneiform ($n = 1$), 2nd metatarsal ($n = 1$), 3rd metatarsal ($n = 1$; Fig. 4), and one nondisplaced fracture of the capitate ($n = 1$; Fig. 5). Out of these, two fractures in one patient were not visible due to higher noise on 3D tomography (Fig. 3), and four fractures in two patients were not visible due to severe artifacts in 3D tomography (motion artifacts (Fig. 4), and an increased noise related to cast fixation (Fig. 5)). No fracture was diagnosed false positive on 3D tomographic images.

Radiographs were available for all but one patient of the hand/wrist group and all patients of the foot/ankle group. Sixteen fractures were missed on radiographs of the hand/wrist (6 triquetrum, 3 trapezium, and one each of the radius,

Table 1 Anatomic location of fractures diagnosed with 3D tomography compared with CT

	Location	3D	CT
Distal upper extremity	Radius	15	15
	Ulna	6	6
	Scaphoid	1	1
	Triquetrum	8*	9
	Pisiform	1	1
	Trapezium	3	3
	Capitate	0*	1
	Hamate	1	1
	2nd metacarpal	0*	1
	4th metacarpal	1	1
	5th metacarpal	3	3
	Proximal phalanx 4th digit	2	2
	Middle phalanx 5th digit	2	2
	Total	43	46
Distal lower extremity	Tibia	4	4
	Fibula	4	4
	Talus	7	7
	Calcaneus	8	8
	Navicular	4	4
	Lateral cuneiform	1*	2
	Cuboid	3	3
	1st metatarsal	1	1
	2nd metatarsal	3*	4
	3rd metatarsal	3*	4
	4th metatarsal	3	3
	5th metatarsal	2	2
	Total	43	46

Data are absolute numbers. Discrepancies between both modalities are marked with an asterisk

ulna, scaphoid, hamate, pisiform, metacarpal, and proximal phalanx), including ten avulsion fractures and six nondisplaced fractures. Seventeen fractures were missed on radiographs of the foot/ankle (6 metatarsals, 4 navicular, 3 calcaneus, 2 lateral cuneiform, 1 tibia, and 1 talus), including 15 avulsion fractures and two nondisplaced fractures.

The interreader reliability for fracture analysis was substantial to almost perfect for the upper ($\kappa = 0.80–0.96$) and lower ($\kappa = 0.70–0.97$) extremity fractures (Table 2).

Qualitative image analysis

Data for qualitative image analysis are presented in Table 3.

Visibility of trabecula, cortices, and soft tissue for the upper and lower distal extremities on 3D tomography and CT was on average rated as good to excellent by both readers; only soft tissue was rated as fair on 3D tomography by reader 2. Noise was rated as good to excellent on both modalities. Overall, image quality was rated as good for 3D tomography and good to excellent for CT. Artifacts were minor on 3D tomography and rated as not present to minor for CT.

Subjective image quality was superior on CT compared with 3D tomography for trabeculae, soft tissue, and artifacts for both readers. Visibility of cortex, noise, and image quality was equal on both modalities for one or both readers (Fig. 6; Table 3).

Subgroup analysis for patients without and with cast revealed significant 3D tomography differences only for reader 1 in the following categories: trabeculae (Likert-scale 1.8 without cast vs. 2.3 with cast; $P = 0.031$), cortex (1.6 vs. 2.1; $P = 0.045$), noise (2.0 vs. 2.7, $P = 0.005$), and image quality (1.6 vs. 2.4; $P = 0.003$). Subgroup analysis for patients without and with cast revealed significant CT differences only for reader 1 in the following categories: trabeculae (Likert-scale 1.4 without cast vs. 1.9 with cast; $P = 0.029$), image quality (1.5 vs. 2.0; $P = 0.013$), and artifacts (1.5 vs. 2.1; $P = 0.034$).

Subgroup analysis for patients without and with external fixation revealed significant 3D tomography differences only for reader 1 in the following categories: trabeculae (Likert-scale 1.7 without external fixation vs. 2.5 with external fixation; $P = 0.036$), and noise (1.9 vs. 2.8; $P = 0.009$). Subgroup analysis for patients without and with external fixation

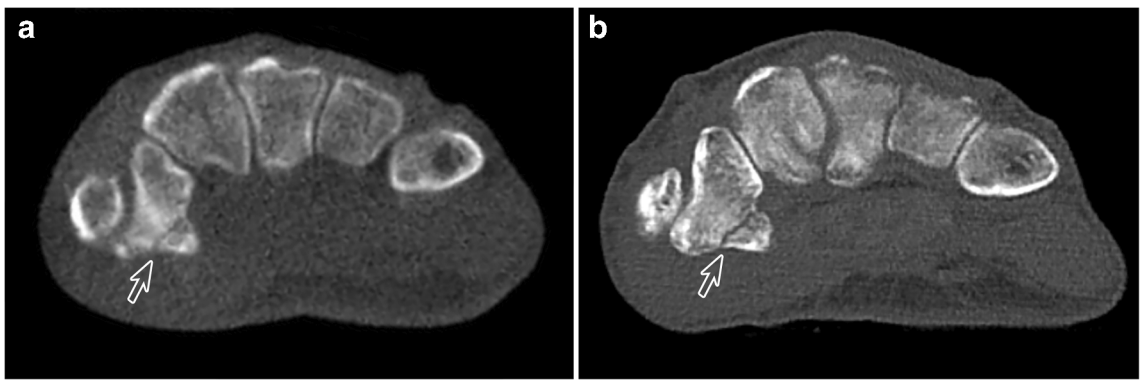

Fig. 1 Fracture presentation of the distal extremities using 3D tomographic twin robotic X-ray compared with CT: right hand of an 83-year-old female with a nondisplaced fracture of the trapezoid tubercle (open arrows) diagnosed on 3D tomography (**a**) and on CT (**b**)

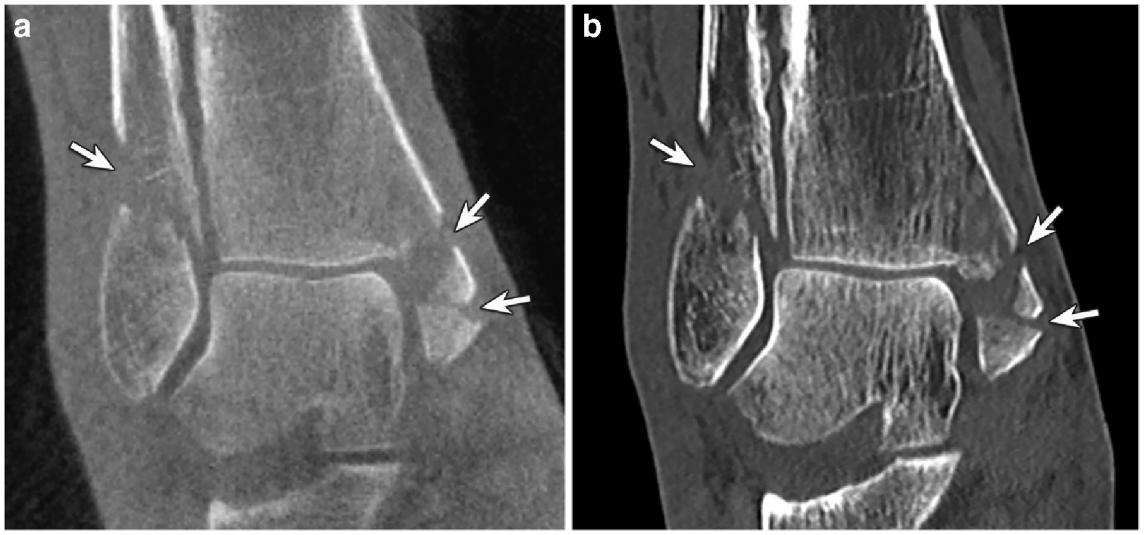

Fig. 2 Fracture presentation of the distal extremities using 3D tomographic twin robotic X-ray compared with CT: right ankle of a 77-year-old female with displaced fractures of both malleoli (arrows) visible using both twin robotic X-ray (**a**) and CT (**b**)

revealed significant CT differences for reader 1 and reader 2 in the following categories: reader 1 trabeculae (Likert-scale 1.4 without external fixation vs. 2.0 with external fixation; $P = 0.022$), reader 1 noise (1.4 vs. 2.0; $P = 0.045$), reader 1 image quality (1.2 vs. 1.8; $P = 0.048$), reader 2 image quality (1.0 vs. 2.0; $P < 0.001$), reader 1 artifacts (1.1 vs. 2.0; $P < 0.001$), and reader 2 artifacts (1.1 vs. 3.0; $P < 0.001$).

Interreader reliability was moderate to (almost) perfect for qualitative analysis of bone and soft tissue structures of the upper ($\kappa = 0.47–0.84$) and lower ($\kappa = 0.48–0.88$) extremities (Table 2).

Radiation exposure analysis

Detailed analysis of radiation exposure is shown in Table 4.

3D tomographies of the distal upper (mean, 19.4 ± 5.9 mGy*cm) and lower (mean, 24.1 ± 11.1 mGy*cm) extremities showed a significantly lower DLP compared with CT (upper extremity: mean, 202.5 ± 72.2 mGy*cm; lower extremity, mean, 141.8 ± 26.7 mGy*cm). Adaptation of the CT-DLP to the 3D scanning range of 23 cm shows an even higher difference (upper extremity: mean, 336.5 ± 52.2 mGy*cm;

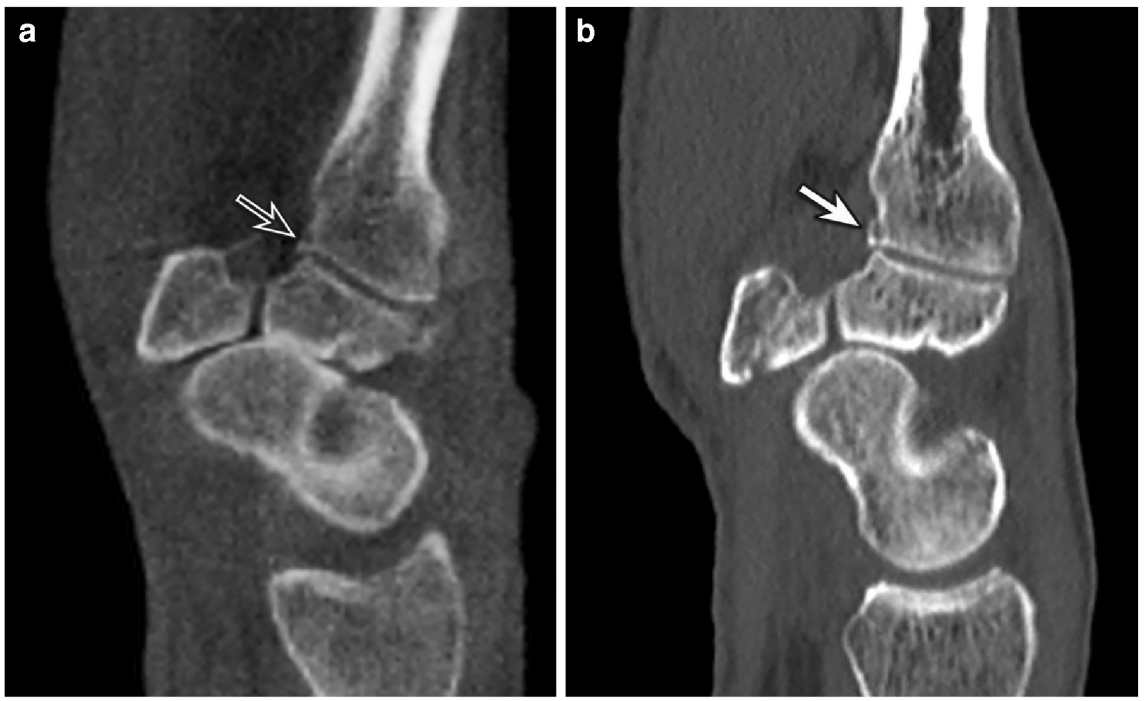

Fig. 3 Left hand of an 83-year-old female with a nondisplaced avulsion fracture at the palmar base of the second metacarpal bone not visible on 3D tomography (open arrow in **a**) but on CT (arrow in **b**)

Fig. 4 Right foot of an 18-year-old male with multiple tarso-metatarsal fractures. The displaced fractures of the navicular and cuboid bone (arrows) were seen on 3D tomography (**a**) and CT images (**b**). Two avulsion fractures at the second and third metatarsal bone were only diagnosed on CT (arrowheads) but missed on 3D tomography due to motion artifacts (black arrowheads)

lower extremity, mean, 182.9 ± 6.5 mGy*cm). Even the highest DLP in 3D tomography was 39.2% of the CT dose (upper extremity: mean, 10.4 ± 4.2%; lower extremity, mean, 17.3 ± 7.8%), and 28.1% of the estimated CT dose of a comparable area of coverage (upper extremity: mean, 5.9 ± 1.9%; lower extremity, mean, 13.1 ± 5.7%).

Discussion

Our study shows that fracture detection on 3D tomography is feasible with only six unrecognized fractures in three patients out of 92 fractures seen on CT. Five of the missed fractures were small avulsion fractures, and one was a nondisplaced fracture of the capitate. In retrospect, the latter fracture was obscured due to cast fixation causing higher noise. However, in none of the other six patients with cast fixation, a fracture was missed.

Overall, the visibility of bone structures, noise, and image quality was rated good on 3D tomography compared with excellent on CT. Only the visibility of soft tissue was rated fair on 3D tomography by reader 2. Despite the slightly reduced image quality, both readers rated image quality to be satisfactory and none rated it insufficient for diagnosis.

Twin robotic X-ray acquires 3D tomographic images in a scanning mode comparable with cone-beam CT. However, this system has only been evaluated by experimental and cadaveric studies [6–9], and the clinical performance of it is yet unknown. Recently Grunz et al. evaluated the system in 16 wrist and 16 ankle cadavers and compared it with CT. They also concluded similar to our study that 3D tomography uses a significantly lower radiation dose than CT with just slightly lower image quality, as well as having more noise and artifacts on 3D tomography. Cone-beam CT is widely used in dentistry and maxillofacial surgery [11–14]. However, only a few studies evaluated extremities [15–20]. Thus, to date and to the best of our knowledge, only five studies investigated acute extremity fractures in comparison with CT [2, 5, 21–23]. One investigated distal radial fractures, but analyzed different patients examined either using cone-beam CT or CT [5] disabling a direct comparison between the two methods. A study by Faccioli et al. investigated finger fractures using both modalities in the same patients [2], showing comparable results with an accuracy of 89.3% to our study (94%). However, our study evaluated not only hand and wrist but also foot and ankle fractures. A third study evaluated extremity fractures using radiography and cone-beam CT and additionally performed a multidetector CT in seven subjects within 30 days of the cone-beam CT [21]. Due to image acquisition of both modalities on the same day in our study, healing and therapeutic effects do not impair our study results. Additionally, we compared a higher number of subjects and fractures in both modalities. The fourth study included a comparison of dose-equivalent radiography, multidetector CT and cone-beam CT on cadaveric wrists with artificially caused fractures [22]. The purpose was to investigate the accuracy of both methods if using an equivalent radiation dose compared with plain radiographs. Therefore, image quality is not comparable

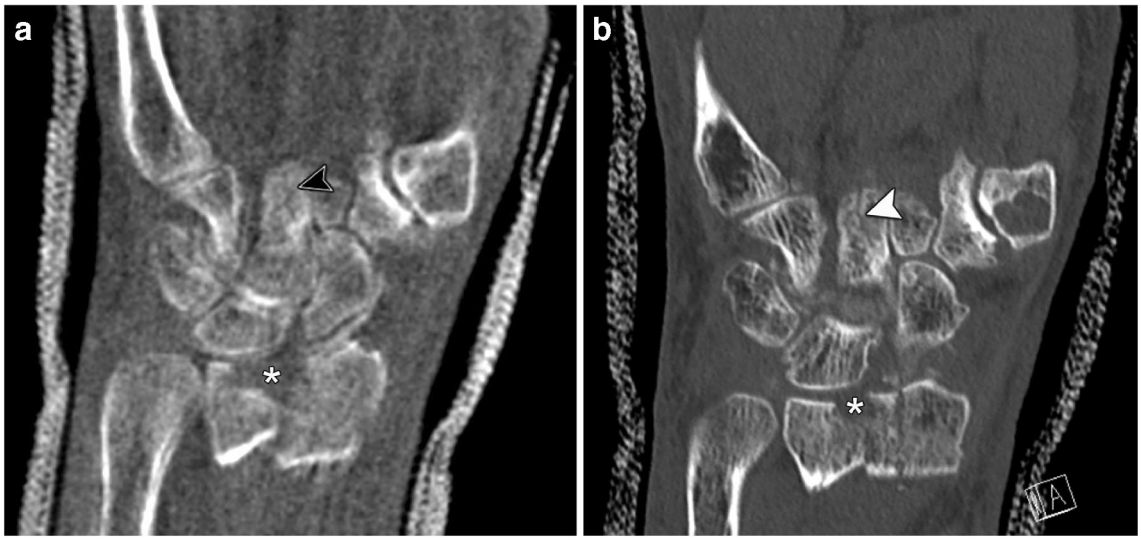

Fig. 5 Left hand in cast fixation of a 76-year-old female imaged with twin robotic X-ray (**a**) and CT (**b**) shows an impacted and displaced radius fracture (asterisk). The additional nondisplaced fracture of the capitate was diagnosed on CT (arrowhead in **b**), but not diagnosed by both readers on 3D tomography (black arrowhead)

with our approach with routine diagnostic CT. The most recent study by Dubreuil et al. examined fewer patients ($n = 36$) with suspected fractures affecting distal extremities or fractures that required preoperative assessment. Similar to our study, each patient underwent cone-beam CT and multislice CT the same day in their study [23]. Due to the smaller number of patients, fewer fractures were evaluated in their study, especially at the lower extremity (37 upper/9 lower extremity vs. 46/46 in our study). However, the authors showed that agreement between cone-beam CT and multislice CT was almost perfect for fracture characterization ($\kappa = 0.94$), which is similar to our comparison of 3D tomography using twin robotic X-ray vs. CT (upper ($\kappa = 0.80$–0.96) and lower ($\kappa = 0.70$–0.97) extremity fractures).

Considering fracture characteristics, we found no false positive fracture. No displaced fracture was missed with 3D

Table 2 Interreader reliability with Cohen's kappa (κ) for fracture analysis and for qualitative evaluation of bone and soft tissue structures of the extremities comparing 3D tomography and CT

Distal upper extremities																
	Anatomic location of fractures								Fracture characteristics							
	Epiphyseal		Metaphyseal		Diaphyseal		Proximal vs. distal		Avulsion		Articular involvement		Mono- vs. multifragmented		Displacement	
	3D	CT	3D	CT	3D	CT	3D	CT	3D	CT	3D	CT	3D	CT	3D	CT
κ	0.96	0.96	0.80	0.82	0.94	0.92	0.92	0.91	0.85	0.85	0.92	0.88	0.89	0.84	0.82	0.83
Distal lower extremities																
	Anatomic location of fractures								Fracture characteristics							
	Epiphyseal		Metaphyseal		Diaphyseal		Proximal vs. distal		Avulsion		Articular involvement		Mono- vs. multifragmented		Displacement	
	3D	CT	3D	CT	3D	CT	3D	CT	3D	CT	3D	CT	3D	CT	3D	CT
κ	0.97	0.94	0.70	0.78	0.85	0.89	0.96	0.95	0.91	0.70	0.89	0.95	0.87	0.82	0.88	0.82
Distal upper extremities																
	Visibility								Overall							
	Trabeculae		Cortex		Soft tissue				Noise		Image quality			Artifacts		
	3D	CT	3D		CT	3D	CT		3D	CT	3D		CT	3D	CT	
κ	0.84	0.73	0.67		0.71	0.47	0.67		0.54	0.61	0.78		0.73	0.47	0.73	
Distal lower extremities																
	Visibility								Overall							
	Trabeculae		Cortex		Soft tissue				Noise		Image quality			Artifacts		
	3D	CT	3D		CT	3D	CT		3D	CT	3D		CT	3D	CT	
κ	0.48	0.73	0.70		0.88	0.48	0.88		0.56	0.70	0.48		0.88	0.76	0.82	

Table 3 Qualitative evaluation of bone and soft tissue structures on a 5-point Likert scale comparing 3D tomography and CT

	Visibility												Overall											
	Trabeculae				Cortex				Soft tissue				Noise				Image quality				Artifacts			
	Reader 1		Reader 2		Reader 1		Reader 2		Reader 1		Reader 2		Reader 1		Reader 2		Reader 1		Reader 2		Reader 1		Reader 2	
	3D	CT	3D	CT	3D	CT	3D	CT	3D	CT	3D	CT	3D	CT	3D	CT	3D	CT	3D	CT	3D	CT	3D	CT
Distal upper extremities																								
Mean	2.0	1.5	2.1	1.0	1.7	1.5	1.1	1.0	2.1	1.6	3.1	1.0	2.2	1.6	1.2	1.0	1.8	1.6	2.0	1.6	2.1	1.6	2.0	1.0
SD	0.6	0.5	0.2	0.0	0.7	0.5	0.2	0.0	0.9	0.6	0.2	0.0	0.7	0.5	0.4	0.0	0.7	0.5	0.0	0.5	0.3	0.7	0.0	0.0
P value	0.013*		< 0.001*		0.157		0.317		0.038*		< 0.001*		0.012*		0.083		0.132		0.008*		0.007*		< 0.001*	
Distal lower extremities																								
Mean	1.9	1.5	2.0	1.0	1.7	1.2	1.1	1.0	2.6	1.2	3.1	1.0	2.1	1.6	1.0	1.0	2.2	1.3	2.0	1.2	2.4	1.3	2.8	1.4
SD	0.7	0.5	0.0	0.0	0.7	0.4	0.2	0.0	0.9	0.4	0.3	0.0	0.6	0.5	0.0	0.0	0.7	0.5	0.0	0.4	0.5	0.5	0.4	0.9
P value	0.035*		< 0.001*		0.021*		0.317		0.001*		< 0.001*		0.020*		1.000		0.001*		< 0.001*		< 0.001*		0.001*	

*$P < 0.05$ was considered statistically significant. The Likert scale was encoded as followed for all criteria but artifacts: 1 = excellent, 2 = good, 3 = fair, 4 = poor, and 5 = inadequate; and for artifacts: 1 = no artifacts, 2 = minor artifacts without influence of image assessment, 3 = moderate artifacts without influence of image assessment (diagnosis still possible), 4 = heavy artifacts with influence of image assessment (only partial diagnosis possible), and 5 = severe artifacts making diagnosis impossible

SD standard deviation

tomography. Fracture evaluation was only limited for the five avulsion fractures missed in our study, which were all small fragments. This is comparable with the study by Faccioli et al. evaluating finger fractures with cone-beam CT and

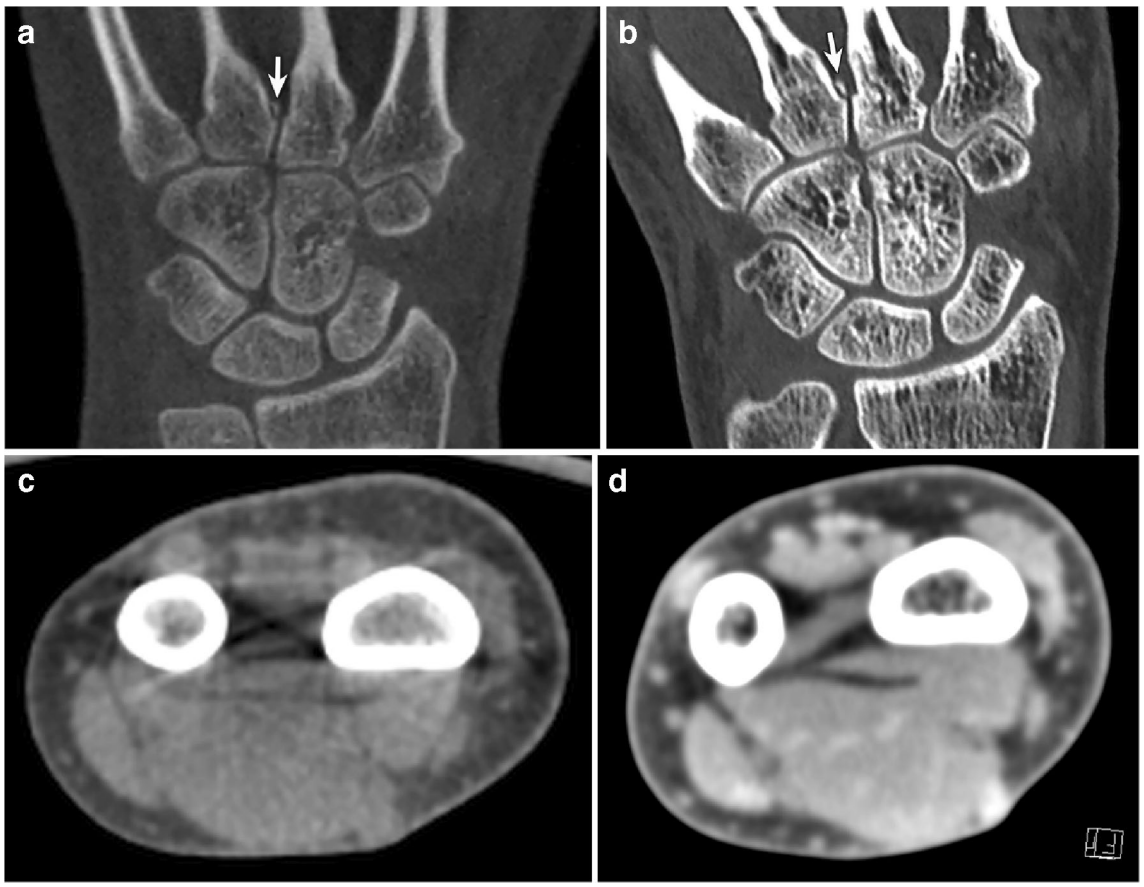

Fig. 6 Left hand of a 46-year-old female shows the image quality in bone (**a** and **b**) and soft tissue resolution (**c** and **d**) using twin robotic X-ray (**a** and **c**) and CT (**b** and **d**). Of note: a nondisplaced avulsion fracture at the fourth metacarpal bone is present (arrows)

Table 4 Comparison of dose length product for upper distal and lower distal extremities using 3D tomography and CT

	3D	CT	CT-DLP adapted to 3D scanning range	Absolute comparison	Comparison adapted to scanning range
DLP of distal upper extremities (mGy*cm)				Percentage of dose in 3D compared with CT (%)	
Mean ± SD	19.4 ± 5.9	202.5 ± 72.2	336.5 ± 52.5	10.4 ± 4.2	5.9 ± 1.9
Minimum	11.0	117.0	168.2	3.6	3.2
Maximum	27.2	379.0	460.0	19.1	11.4
P value	< 0.001*				
DLP of distal lower extremities (mGy*cm)				Percentage of dose in 3D compared with CT (%)	
Mean ± SD	24.1 ± 11.1	141.8 ± 26.7	182.9 ± 6.5	17.3 ± 7.8	13.1 ± 5.7
Minimum	14.1	103.0	173.1	9.5	7.7
Maximum	56.0	213.0	199.3	39.2	28.1
P value	< 0.001*				

*$P < 0.05$ was considered statistically significant

DLP dose length product, *SD* standard deviation

conventional CT, where cone-beam CT was less accurate than CT in depicting small bone fragments [2]. A reason for the missed fractures in our study might be that 3D tomography with twin robotic X-ray is more prone to noise, cone-beam and motion artifacts. This is due to the volumetric acquisition process of a twin robotic X-ray system with motion artifacts occurring in the entire image volume.

Subjective image quality of CT was rated mostly excellent compared with good at 3D tomography, except for soft tissue depiction that was rated as fair to good. Studies have shown that image quality of cone-beam CT compared with conventional CT is variable with equivalent to superior or inferior results [5, 24, 25]. Cone-beam CT has been described as more prone to artifacts than CT in analysis of distal radius fractures [5]. This is because CT scanners are better adjusted for corrections of beam-hardening and iterative reconstruction [26]. Demehri et al. showed that cone-beam CT has a favorable bone but inferior soft tissue resolution compared with multidetector CT [24], which is in line with our results. Since soft tissue depiction plays an inferior role in fracture diagnosis, we believe an inferior soft tissue resolution is negligible considering this diagnosis. A cadaveric study evaluated bone and soft tissue performance of the twin robotic X-ray system for the lumbar spine [7]. The study concluded that depiction of bone is comparable with CT in specimens with a BMI of up to 30 kg/m^2. However, soft tissue structure depiction was limited in comparison with CT regardless of the BMI. Further cone-beam CT studies showed these limitations for the trunk as well, e.g. limited detection of low-contrast objects, and higher susceptibility to motion artifacts especially of the chest, due to the longer image acquisition time compared with CT [27, 28]. Additionally, the cross-sectional field-of-view of these units compared with CT is limited to 23 cm for the twin robotic X-ray unit. Thus, the region of interest needs to be centered.

The radiation dose on 3D tomography was markedly lower compared with CT, which is in line with prior investigations [2, 21, 25, 29–31]. The higher radiation dose on CT is most likely the reason for the slightly better CT performance in subjective image quality in our study. We believe that an increase of radiation dose on 3D tomography might have allowed detection of the missed fractures. This could increase image quality and might be taken into consideration for further clinical implementation.

Limitations of our study are as follows: The fractures we analyzed showed a wide range of variability. Thus, a comparison with the clinical outcome was not feasible. However, our goal was to investigate the overall diagnostic value of fractures using this low-dose 3D tomography technique. We analyzed fractures first using CT and added a 3D tomography if a fracture was present. Therefore, a selective bias might have been present, and an investigation first using twin robotic X-ray followed by CT might be of interest. Additionally, this might have introduced a selection bias priming the readers for fracture detection since all patients included had minimum one fracture. Furthermore, we only evaluated acute fractures. Thus, we cannot report the accuracy of fracture healing analysis. Our study did not include a control group of non-fractured patients due to radiation protection. No intrareader reliability was performed. The 3D scanning field of the system is limited to 23 cm, which might limit the assessment of extensive longitudinal extremity fractures. Our study results can only be applied to the 3D tomography system of the investigated twin robotic X-ray unit and not necessarily to other 3D fluoroscopy or cone-beam CT units, e.g. due to different acquisition techniques and reconstruction algorithms, which make a direct comparison difficult. Also, these results only reflect the performance of the twin robotic X-ray system for distal extremity fractures. However, the diagnostic performance at other regions still needs to be evaluated.

Conclusion

Fracture assessment of peripheral extremities is reliable utilizing a low-dose 3D tomography X-ray system, despite mildly impaired image quality. Thus, 3D tomography is a reliable alternative to CT for wrist and ankle fracture diagnostics and has the potential benefit of workflow optimization with its multipurpose technology.

Acknowledgments The authors kindly thank Johannes Voigt (Siemens Healthineers, Erlangen, Germany) for calculating the dose-length product.

Funding information The Department of Radiology and Nuclear Medicine (University Hospital Basel, Switzerland) received a financial research grant by Siemens Healthineers.

Compliance with ethical standards

Ethical approval All procedures performed in studies involving human participants were in accordance with the ethical standards of the institutional and/or national research committee and with the 1964 Helsinki declaration and its later amendments or comparable ethical standards.

References

1. Badia A, Riano F, Ravikoff J, Khouri R, Gonzalez-Hernandez E, Orbay JL. Dynamic intradigital external fixation for proximal interphalangeal joint fracture dislocations. J Hand Surg Am. 2005;30(1):154–60.
2. Faccioli N, Foti G, Barillari M, Atzei A, Mucelli RP. Finger fractures imaging: accuracy of cone-beam computed tomography and multislice computed tomography. Skelet Radiol. 2010;39(11):1087–95.
3. Heuck A, Bonel H, Stabler A, Schmitt R. Imaging in sports medicine: hand and wrist. Eur J Radiol. 1997;26(1):2–15.
4. Zbijewski W, De Jean P, Prakash P, Ding Y, Stayman JW, Packard N, et al. A dedicated cone-beam CT system for musculoskeletal extremities imaging: design, optimization, and initial performance characterization. Med Phys. 2011;38(8):4700–13.
5. Lang H, Neubauer J, Fritz B, Spira EM, Strube J, Langer M, et al. A retrospective, semi-quantitative image quality analysis of cone beam computed tomography (CBCT) and MSCT in the diagnosis of distal radius fractures. Eur Radiol. 2016;26(12):4551–61.
6. Benz RM, Garcia MA, Amsler F, Voigt J, Fieselmann A, Falkowski AL, et al. Initial evaluation of image performance of a 3-D x-ray system: phantom-based comparison of 3-D tomography with conventional computed tomography. J Med Imaging (Bellingham). 2018;5(1):015502.
7. Benz RM, Harder D, Amsler F, Voigt J, Fieselmann A, Falkowski AL, et al. Initial assessment of a prototype 3D cone-beam computed tomography system for imaging of the lumbar spine, evaluating human cadaveric specimens in the upright position. Invest Radiol. 2018.
8. Grunz JP, Gietzen CH, Kunz AS, Weng AM, Veyhl-Wichmann M, Ergun S, et al. Twin robotic X-ray system for 3D cone-beam CT of the wrist: an evaluation of image quality and radiation dose. AJR Am J Roentgenol. 2020;214(2):422–7.
9. Grunz JP, Kunz AS, Gietzen CH, Weng AM, Veyhl-Wichmann M, Ergun S, et al. 3D cone-beam CT of the ankle using a novel twin robotic X-ray system: assessment of image quality and radiation dose. Eur J Radiol. 2019;119:108659.
10. Viera AJ, Garrett JM. Understanding interobserver agreement: the kappa statistic. Fam Med. 2005;37(5):360–3.
11. Guerrero ME, Jacobs R, Loubele M, Schutyser F, Suetens P, van Steenberghe D. State-of-the-art on cone beam CT imaging for preoperative planning of implant placement. Clin Oral Investig. 2006;10(1):1–7.
12. Verweij JP, Anssari Moin D, Wismeijer D, van Merkesteyn JPR. Replacing heavily damaged teeth by third molar autotransplantation with the use of cone-beam computed tomography and rapid prototyping. J Oral Maxillofac Surg. 2017.
13. Oliveira GQV, Rossi MA, Vasconcelos TV, Neves FS, Crusoe-Rebello I. Cone beam computed tomography assessment of the pterygomaxillary region and palatine canal for Le Fort I osteotomy. Int J Oral Maxillofac Surg. 2017.
14. von Arx T, Antonini L, Salvi GE, Bornstein MM. Changes of periodontal parameters after apical surgery: correlation of clinical and cone-beam computed tomographic data. J Endod. 2017;43(6):876–84.
15. De Cock J, Mermuys K, Goubau J, Van Petegem S, Houthoofd B, Casselman JW. Cone-beam computed tomography: a new low dose, high resolution imaging technique of the wrist, presentation of three cases with technique. Skelet Radiol. 2012;41(1):93–6.
16. Finkenstaedt T, Morsbach F, Calcagni M, Vich M, Pfirrmann CW, Alkadhi H, et al. Metallic artifacts from internal scaphoid fracture fixation screws: comparison between C-arm flat-panel, cone-beam, and multidetector computed tomography. Investig Radiol. 2014;49(8):532–9.
17. Carrino JA, Al Muhit A, Zbijewski W, Thawait GK, Stayman JW, Packard N, et al. Dedicated cone-beam CT system for extremity imaging. Radiology. 2014;270(3):816–24.
18. Hirschmann A, Pfirrmann CW, Klammer G, Espinosa N, Buck FM. Upright cone CT of the hindfoot: comparison of the non-weight-bearing with the upright weight-bearing position. Eur Radiol. 2014;24(3):553–8.
19. Hirschmann A, Buck FM, Fucentese SF, Pfirrmann CW. Upright CT of the knee: the effect of weight-bearing on joint alignment. Eur Radiol. 2015;25(11):3398–404.
20. Hirschmann A, Buck FM, Herschel R, Pfirrmann CW, Fucentese SF. Upright weight-bearing CT of the knee during flexion: changes of the patellofemoral and tibiofemoral articulations between 0 degrees and 120 degrees. Knee Surg Sports Traumatol Arthrosc. 2017;25(3):853–62.
21. Huang AJ, Chang CY, Thomas BJ, MacMahon PJ, Palmer WE. Using cone-beam CT as a low-dose 3D imaging technique for the extremities: initial experience in 50 subjects. Skelet Radiol. 2015;44(6):797–809.
22. Neubauer J, Benndorf M, Reidelbach C, Krauss T, Lampert F, Zajonc H, et al. Comparison of diagnostic accuracy of radiation dose-equivalent radiography, multidetector computed tomography and cone beam computed tomography for fractures of adult cadaveric wrists. PLoS One. 2016;11(10):e0164859.
23. Dubreuil T, Mouly J, Ltaief-Boudrigua A, Martinon A, Tilhet-Coartet S, Tazarourte K, et al. Comparison of cone-beam computed tomography and multislice computed tomography in the assessment of extremity fractures. J Comput Assist Tomogr. 2019;43(3):372–8.
24. Demehri S, Muhit A, Zbijewski W, Stayman JW, Yorkston J, Packard N, et al. Assessment of image quality in soft tissue and bone visualization tasks for a dedicated extremity cone-beam CT system. Eur Radiol. 2015;25(6):1742–51.
25. Liang X, Jacobs R, Hassan B, Li L, Pauwels R, Corpas L, et al. A comparative evaluation of cone beam computed tomography (CBCT) and multi-slice CT (MSCT): part I. On subjective image quality. Eur J Radiol. 2010;75(2):265–9.

26. Barrett JF, Keat N. Artifacts in CT: recognition and avoidance. Radiographics. 2004;24(6):1679–91.
27. Schegerer AA, Lechel U, Ritter M, Weisser G, Fink C, Brix G. Dose and image quality of cone-beam computed tomography as compared with conventional multislice computed tomography in abdominal imaging. Investig Radiol. 2014;49(10):675–84.
28. Zhang Q, Hu YC, Liu F, Goodman K, Rosenzweig KE, Mageras GS. Correction of motion artifacts in cone-beam CT using a patient-specific respiratory motion model. Med Phys. 2010;37(6):2901–9.
29. Coppenrath E, Draenert F, Lechel U, Veit R, Meindl T, Reiser M, et al. Cross-sectional imaging in dentomaxillofacial diagnostics: dose comparison of dental MSCT and NewTom 9000 DVT. Rofo. 2008;180(5):396–401.
30. Roberts JA, Drage NA, Davies J, Thomas DW. Effective dose from cone beam CT examinations in dentistry. Br J Radiol. 2009;82(973):35–40.
31. Loubele M, Bogaerts R, Van Dijck E, Pauwels R, Vanheusden S, Suetens P, et al. Comparison between effective radiation dose of CBCT and MSCT scanners for dentomaxillofacial applications. Eur J Radiol. 2009;71(3):461–8.